Soliton formation to study the dynamical behaviour of biological evolution model

Ghazala Akram [*], Saima Arshed [†], Maasoomah Sadaf [‡] and Zainab [§]

Keywords: Soliton solutions; Fractional Peyrard-Bishop DNA model; Jacobi elliptic function; The tanh-coth expansion method ; Painlevé test

Abstract

This article investigates the fractional Peyrard-Bishop DNA model. The construction of soliton solutions have been successfully obtained by utilizing two versatile analytical methods, namely, the Jacobi elliptic function method and the tanh-coth method. Furthermore, the Painlevé test (P-test) has been employed on the proposed model for investigating integrability. The proposed model is proved to be integrable. Some of the obtained solutions have been examined graphically to study the dynamical behavior.

1 Introduction

The topic fractional calculus has gained considerable interest among the researchers in the last few decades, because of its capability of solving problems of complex nature in science and engineering fields. The 1st international conference on fractional calculus, held in in 1974, had played a vital role in the development of this branch of mathematics. Many mathematicians, for instance; Lagrange, Abel, Euler, Liouville, Riemann, Caputo, Mainardi and many others have played a prominent role in the development of fractional calculus. Riemann-Liouville, Caputo-Hadamard, Erdlyi-Kober, Katugampola and Weyl [8, 10, 12, 20] have introduced different fractional derivatives and integrals that have been very useful to tackle with different complex problems. The beta-derivative [4] is used to solve Hunter-Saxton equation. The non-local form of the Atangana beta-derivative is presented by [16]. The M-fractional derivative was introduced in [25].

Many physical phenomena in mechanics, viscoplasticity, optics, biology and visco-fluid dynamics are modeled by fractional partial differential equations. Therefore, a number of versatile techniques have been introduced by different researchers to solve such fractional partial differential equations. Bibi *et al.* extracted exact solutions for fractional STO and $(3+1)$-dimensional KdV-ZK equation via the $(\frac{G'}{G^2})$-expansion method. The modified Riemann-Liouville fractional derivative [5] is used to examine the fractional effects of the proposed model. Mohyud-Din extracted solutions for space-time fractional Zakharov Kuznetsov Benjamin Bona Mahony (ZKBBM) equation and fractional coupled Burgers equation using the $(\frac{G'}{G^2})$-expansion method [15]. Rizvi *et al.* obtained the exact soliton

[*]Department of Mathematics, University of the Punjab, Lahore 54590, Pakistan. Email: toghazala2003@yahoo.com
[†]Department of Mathematics, University of the Punjab, Lahore 54590, Pakistan. Email: saima.math@pu.edu.pk
[‡]Department of Mathematics, University of the Punjab, Lahore 54590, Pakistan. Email: maasoomah.math@pu.edu.pk
[§]Department of Mathematics, University of the Punjab, Lahore 54590, Pakistan. Email: zainabimran2216@gmail.com

solutions of $(2+1)$-dimensional fractional Schrödinger equation via F-expansion and improved F-expansion method [21].
The main purpose of this work is the extraction of soliton solutions of the fractional Peyrard-Bishop DNA model. The exact soliton solutions are constructed using the Jacobi elliptic function method (JEFM) and the tanh-coth expansion method. The fractional effects on the soliton solutions are studied for two kinds of fractional derivatives, namely, the β-derivative and M-truncated derivative. The proposed methods are very effective and reliable for finding soliton solutions of nonlinear partial differential equations (NLPDEs). Biswas *et al.* obtained new soliton solutions using extended JEFM [6]. Liu *et al.* constructed new exact solutions for the nonlinear wave equation [13]. Parkes used the tanh-coth expansion method for finding solutions to nonlinear evolution equations [18].
The Painlevé-test has also been employed on the governing equation for the first time in this paper. The Painlevé-test is an approach used for testing the integrability of NLPDEs.
Peyrard and Bishop were the first to explore distortion of the DNA double helix [19]. Whereas, the local opening of DNA helix during transcription, dynamic DNA helicoidal Peyrard-Bishop model has been studied by Slobodan Zdravkovic [27]. Moreover, Filip and Nicolas have discussed solitons in the Peyrard-Bishop model of a DNA molecule via renormalization group [7]. Recently, the proposed model has been examined by employing different analytical techniques [2, 3, 11, 14, 26] and bright soliton, dark soliton, singular soliton, combo soliton and periodic solutions are reported.
The Morse expressed the Peyrard-Bishop model of DNA equation in Hamiltonian form, as

$$\zeta_p\left(\phi_q - l_q\right) = \vartheta\left(e^{-\varepsilon(\phi_q - l_q)} - 1\right)^2, \tag{1.1}$$

where $\zeta_p\left(\phi_q - l_q\right)$ represents the Morse's potential, the shortest distance between nucleotides is expressed by ϕ_q and l_q, whereas Morse's potential depth and width are ϑ and ε respectively. The Hamiltonian for DNA strings are also defined by Zdarvkovic [27] and then enhanced by Dauxois [9]. The Hamiltonian of the hydrogen bonds for the strings perforation can be specified, as [1, 3, 17]

$$\begin{aligned} H(\phi) &= \frac{1}{2p}\alpha_q^2 + \frac{\beta_1}{2}\Delta^2\phi_q + \frac{\beta_2}{4}\Delta^4\phi_q + \nu\left(e^{-\varepsilon\sqrt{2}\phi_b}\right), \\ \Delta\phi_q &= \phi_{q+1} - \phi_q, \end{aligned} \tag{1.2}$$

where $\alpha_q = p\phi_q$ is the momentum, β_1 and β_2 represents the strength for the nonlinear and linear bond and ν is an arbitrary constant. The mathematical model of (1.2) is as follow:

$$\phi_{tt} - (\delta_1 + 3\delta_2\phi_x^2)\phi_{xx} - 2\lambda\ \rho e^{-\lambda\phi}\left(e^{-\lambda\phi} - 1\right) = 0, \tag{1.3}$$

where $\delta_1 = \frac{\beta_1}{p}d^2$, $\delta_2 = \frac{\beta_2}{p}d^4$, $\rho = \frac{\nu}{p}$, $\lambda = \sqrt{2}\varepsilon$ and d is the inter-site nucleotide distance in the DNA strands [3, 17].
In **β-fractional derivative**, the proposed model has the following form.

$$D_t^{2\gamma}\phi - \left(\delta_1 + 3\delta_2\left(D_x^{\gamma}\phi\right)^2\right)D_x^{2\gamma}\phi - 2\lambda\rho e^{-\lambda\phi}\left(e^{-\lambda\phi} - 1\right) = 0, \tag{1.4}$$

where $D_t^{2\gamma}$ is β-fractional derivative.
The dynamical model in **M-fractional derivative** has the following form.

$$D_{M,t}^{2\gamma,\beta}\phi - (\delta_1 + 3\delta_2(D_{M,x}^{\gamma,\beta})^2)D_{M,x}^{2\gamma,\beta}\phi - 2\lambda\rho e^{-\lambda\phi}(e^{-\lambda\phi} - 1) = 0, \tag{1.5}$$

where $D_{M,t}^{\gamma,\beta}$ *and* $D_{M,x}^{\gamma,\beta}$ are the M-fractional derivatives.

The article is organized as follows: Section 2, contains the preliminaries. In Section 3, the algorithm of Jacobi elliptic function expansion method has been explained. Section 4 describes the tanh-coth

method. Section 5 includes the mathematical analysis of the model and the solution obtained by proposed methods. The algorithmic steps of Painlevé test has been described in Section 6. Moreover, in Section 7, the P-test has been employed on Peyrard-Bishop DNA model. Section 8 presents the graphically illustrations of some constructed solutions. The concluding remarks are presented in Section 9.

2 Preliminaries

The definitions of fractional derivatives along with their fundamental properties are discussed in this section.

2.1 β-derivative and its properties

Definition 1 Another kind of conformable derivative known as β-fractional derivative can be defined, as [4]

$$ {}_0^B D_x^\gamma g(x) = \lim_{\varepsilon \to 0} \frac{g\left(x + \varepsilon \left(x + \frac{1}{\Gamma(\gamma)}\right)^{1-\gamma}\right) - g(x)}{\varepsilon}, \quad 0 < \gamma < 1. $$

β-derivative have the following properties [4, 16].

$$ \begin{aligned} {}_0^B D_x^\gamma \left(rg(x) + sh(x)\right) &= r\, {}_r^B D_x^\gamma g(x) + s\, {}_s^B D_x^\gamma h(x), \quad \forall r, s \in \Re \\ {}_0^B D_x^\gamma \left(g(x) * h(x)\right) &= h(x) {}_r^B D_x^\gamma g(x) + g(x) {}_r^B D_x^\gamma h(x), \\ {}_0^B D_x^\gamma \left\{\frac{g(x)}{h(x)}\right\} &= \frac{h(x) {}_r^B D_x^\gamma g(x) - g(x) {}_r^B D_x^\gamma h(x)}{h^2(x)}, \\ {}_0^B D_x^\gamma c &= 0, \quad \text{for } c \text{ any constant.} \end{aligned} $$

2.2 M-truncated derivative

M-truncated derivative, M-truncated integral and their properties have been defined in this section.
Definition 2 Suppose $g : [r, \infty) \to \Re$ and $x > 0$. Also $0 < \gamma < 1$ and $\tau > 0$. The M-truncated derivative of g of order γ is represented by ${}_j^M D^{\gamma,\tau}$ and defined, as [24]

$$ {}_j^M D^{\gamma,\tau} g(x) = \lim_{\varepsilon \to 0} \frac{g\left(x\, {}_jE_\tau(\varepsilon x^{-\gamma})\right) - g(x)}{\varepsilon}, $$

$\forall\, t > 0$, where ${}_iE_\tau(.)$, $\tau > 0$ is a truncated Mittag-Leffler function of one parameter defined, as

$$ {}_jE_\tau(x) = \sum_{k=0}^{j} \frac{x^k}{\Gamma(\tau k + 1)}. $$

The M-truncated derivative have the following properties [23]. Suppose $0 < \gamma < 1$, $\tau > 0$, $r,\ s \in \Re$ and $g,\ h$ are γ-differentiable at $x > 0$.

$$ {}_j^M D^{\gamma,\tau}(rg + sh)(x) = r\, {}_j^M D^{\gamma,\tau} g(x) + s\, {}_j^M D^{\gamma,\tau} h(x), $$

$$ {}_j^M D^{\gamma,\tau}(g * h) = g(x) {}_j^M D^{\gamma,\tau} h(x) + h(x) {}_j^M D^{\gamma,\tau} g(x), $$

$$ {}_j^M D^{\gamma,\tau}\left(\frac{g}{h}\right)(x) = \frac{h(x) {}_j^M D^{\gamma,\tau} g(x) - g(x) {}_j^M D^{\gamma,\tau} h(x)}{h(x)^2}, $$

$$ {}_{j}^{M}D^{\gamma,\tau}(c) = 0, \quad \text{where} g(x) = c, \text{is a constant.}$$

The chain rule of M-truncated derivative for a differentiable function is defined, as

$$ {}_{j}^{M}D^{\gamma,\tau}\left(g(x)\right) = \frac{x^{1-\gamma}}{\Gamma[\tau+1]}\frac{dg(x)}{dx}.$$

3 Jacobi elliptic function method (JEFM)

The algorithm of JEFM is given as follows:
Step 1 The NLPDE is considered, as

$$P\left(\phi, \phi_x, \phi_t, \phi_{xx}, \phi_{xt}, \phi_{tt}, \ldots\right) = 0, \tag{3.1}$$

where $\phi = \phi(x,t)$.
Step 2 The NLPDE is converted into the following ordinary differential equation by employing wave transformation

$$Q(u, u', u'', ...) = 0, \tag{3.2}$$

where $'$ denotes $\frac{d}{d\xi}$.
Step 3 The solution of $u(\xi)$ is assumed in the form,

$$u(\xi) = \sum_{k=0}^{N} A_k(\theta(\xi))^k \tag{3.3}$$

and

$$u'(\xi) = \sum_{k=1}^{N} kA_k(\theta(\xi))^{(k-1)}(\theta'(\xi)). \tag{3.4}$$

The value of $\theta(\xi)$ can be considered, as

$$\theta(\xi) = sn(p\xi, m) \tag{3.5}$$

or

$$\theta(\xi) = cn(p\xi, m) \tag{3.6}$$

or

$$\theta(\xi) = dn(p\xi, m), \tag{3.7}$$

where m represents the modulus of ellipticity. For $m \to 1$ or $m \to 0$, the JE function assumes values that are illustrated in Table 1. **Step 4** N is determined by balancing principle. The Eq.(3.3) is

Table 1: Jacobi elliptic (JE) functions

Function	$m \to 0$	$m \to 1$
$sn(p\xi, m)$	$\sin(p\xi)$	$\tanh(p\xi)$
$cn(p\xi, m)$	$\cos(p\xi)$	$sech(p\xi)$
$dn(p\xi, m)$	1	$sech(p\xi)$

inserted along with the derivatives in the Eq.(3.2). Afterwards, assembling all the coefficients of the powers of $\theta(\xi)$ and putting them equal to zero, a set of algebraic equations is obtained. Then, by solving the obtained system, the values of required arbitrary parameters *i.e.* $A_k,\ k = 1,\ 2, ...,\ N$ are determined.

4 The tanh-coth expansion method

The algorithm of tanh-coth expansion method is as follow:
Step 1 The Eq.(3.1) and Eq.(3.2) are considered.
Step 2 The solution of $u(\xi)$ is assumed as follow:

$$u(\xi) = \sum_{k=0}^{N} A_k(\theta(\xi))^k + \sum_{k=1}^{N} B_k(\theta(\xi))^{-k}. \tag{4.1}$$

The derivative is defined, as

$$\frac{d}{d\xi} = m(1-\theta^2(\xi))\frac{d}{d\theta}, \tag{4.2}$$

where m is an arbitrary constant and $\theta(\xi)$ can be considered, as

$$\theta(\xi) = \tanh(\xi) \tag{4.3}$$

or

$$\theta(\xi) = \coth(\xi). \tag{4.4}$$

Step 3 N is measured by balancing principle. The Eq.(4.1) is inserted along with the derivatives in the Eq.(3.2). Afterwards, assembling all the coefficients of the powers of $\theta(\xi)$ and putting them equal to zero, a system of algebraic equations is obtained. By solving the obtained system, the values of required arbitrary parameters *i.e.* A_k and B_k, $k = 1, 2, ..., N$ are determined.

5 Mathematical analysis of the proposed model

For the extraction of the exact solutions of Eq.(1.3), the transformation

$$\phi(x,t) = U(\xi), \tag{5.1}$$

have been employed.
The parameter ξ is defined in two ways, as

$$\begin{aligned} \xi &= \frac{1}{\gamma}\left(x + \frac{1}{\Gamma(\gamma)}\right)^{\gamma} - \frac{\mu}{\gamma}\left(t + \frac{1}{\Gamma(\gamma)}\right)^{\gamma}, \quad (\beta - \textbf{derivative}), \\ \xi &= \frac{\Gamma(\tau+1)}{\gamma}(x^{\gamma} - \mu t^{\gamma}), \qquad (\mathbf{M} - \textbf{truncatedderivative}). \end{aligned} \tag{5.2}$$

Here μ represents the speed of traveling wave and ξ is the traveling wave's amplitude. Utilizing the transformation Eq.(5.1) together with Eq.(5.2), the obtained ordinary differential equation is

$$\mu^2(U'') - (\delta_1 + 3\delta_2(U'^2)U'' - 2\lambda\rho e^{-\lambda U}(e^{-\lambda U} - 1) = 0. \tag{5.3}$$

Multiplying Eq.(5.3) by U' and integrating the obtained equation implies

$$\frac{(\mu^2 - \delta_1)}{2}(U')^2 - \frac{3}{4}\delta_2(U')^4 + \rho e^{-\lambda U}(e^{-\lambda U} - 2) + C = 0. \tag{5.4}$$

Here C is the constant of integration.
Taking

$$u(\xi) = e^{-\lambda U(\xi)} \tag{5.5}$$

and putting Eq.(5.5) into Eq.(5.4), the above expression becomes

$$\frac{(\mu^2 - \delta_1)}{2\lambda^2}u^2(u')^2 - \frac{3}{4\lambda^4}\delta_2(u')^4 + \rho u^5(u-2) + Cu^4 = 0. \tag{5.6}$$

The Eq.(5.6) is solved in the following subsections.

5.1 The Jacobi elliptic method

Balancing principle gives $N = 2$, then Eq.(3.3) can be written, as

$$u(\xi) = A_0 + A_1\theta(\xi) + A_2\theta^2(\xi), \tag{5.7}$$

where A_0, A_1 and A_2 are the arbitrary parameters to be determined. The Eq.(5.7) is inserted along with the derivatives in Eq.(5.6). By assembling all the coefficients of $\theta(\xi)$ and equating them to zero, leads to the construction of a system of algebraic equations. After solving the system with mathematica aid, the following cases have been obtained.

Case 1 For $\theta(\xi) = sn(p\xi, m)$

By employing the proposed technique the following values of parameters have been obtained.

$$\begin{aligned} A_0 &= \mp\frac{2\sqrt{3\delta_2}m^2}{\lambda^2\sqrt{\rho}}, \qquad A_1 = 0, \\ A_2 &= \mp\frac{2\sqrt{3\delta_2}m^2}{\lambda^2\sqrt{\rho}}, \qquad \mu = \mp\frac{\sqrt{-6\delta_2\lambda^2\sqrt{\rho} - \sqrt{3}\left(\lambda^2\delta_1 + 12m^2\delta_2\right)}}{\sqrt[4]{3}\lambda}, \\ C &= -\frac{4\left(\sqrt{3\delta_2}m^2\lambda^2\sqrt{\rho} + 3m^4\delta_2\right)}{\lambda^4}. \end{aligned} \tag{5.8}$$

Inserting Eq.(5.8) into Eq.(5.7) yields,

$$u(\xi) = \mp\frac{2\sqrt{3\delta_2}m^2\left(-1 + sn(p\xi, m)^2\right)}{\lambda^2\sqrt{\rho}}. \tag{5.9}$$

The obtained result for Eq.(1.3) is

$$\phi(x,t) = -\frac{1}{\lambda}\ln\left[\mp\frac{2\sqrt{3\delta_2}m^2\left(-1 + sn(p\xi, m)^2\right)}{\lambda^2\sqrt{\rho}}\right]. \tag{5.10}$$

For $n \to 1$, the Eq.(5.10) becomes

$$\phi(x,t) = -\frac{1}{\lambda}\ln\left[\mp\frac{2\sqrt{3\delta_2}m^2 sech^2(p\xi)}{\lambda^2\sqrt{\rho}}\right], \quad \rho > 0, \delta_2 > 0. \tag{5.11}$$

Eq.(5.11) presents the bright soliton solution for the governing model.

Case 2 For $\theta(\xi) = cn(p\xi, m)$

By employing the proposed technique the following values of parameters have been obtained.

$$\begin{aligned} A_0 &= 0, \qquad A_1 = 0, \\ A_2 &= \mp\frac{2\sqrt{3\delta_2}m^2}{\lambda^2\sqrt{\rho}}, \qquad \mu = \mp\frac{\sqrt{6\delta_2\lambda^2\sqrt{\rho} + \sqrt{3}\left(\lambda^2\delta_1 + 12m^2\delta_2\right)}}{\sqrt[4]{3}\lambda}, \\ C &= -\frac{4\left(\sqrt{3\delta_2}m^2\lambda^2\sqrt{\rho} + 3m^4\delta_2\right)}{\lambda^4}. \end{aligned} \tag{5.12}$$

Inserting Eq.(5.12) into Eq.(5.7) yields,

$$u(\xi) = \mp\frac{2\sqrt{3\delta_2}m^2\left(cn(p\xi, m)^2\right)}{\lambda^2\sqrt{\rho}}. \tag{5.13}$$

The result obtained for Eq.(1.3) is

$$\phi(x,t) = -\frac{1}{\lambda}\ln\left[\mp\frac{2\sqrt{3\delta_2}m^2\left(cn(p\xi, m)^2\right)}{\lambda^2\sqrt{\rho}}\right]. \tag{5.14}$$

For $n \to 1$, the Eq.(5.14) becomes

$$\phi(x,t) = -\frac{1}{\lambda}\ln\left[\mp\frac{2\sqrt{3\delta_2}m^2 sech^2(p\xi)}{\lambda^2\sqrt{\rho}}\right], \tag{5.15}$$

with constraint condition, $\rho > 0$ and $\delta_2 > 0$.
Case 3 For $\theta(\xi) = dn(p\xi, m)$
By employing the proposed technique the following values of parameters have been obtained.

$$\begin{aligned} A_0 &= \mp\frac{2\sqrt{3\delta_2}m^2}{\lambda^2\sqrt{\rho}}, \qquad A_1 = 0, \\ A_2 &= \mp\frac{2\sqrt{3\delta_2}m^2}{\lambda^2\sqrt{\rho}}, \qquad \mu = \mp\frac{\sqrt{6\delta_2\lambda^2\sqrt{\rho} - \sqrt{3}\left(-\lambda^2\delta_1 + 12m^2\delta_2\right)}}{\sqrt[4]{3}\lambda}, \\ C &= \frac{4\left(\sqrt{3\delta_2}m^2\lambda^2\sqrt{\rho} - 3m^4\delta_2\right)}{\lambda^4}. \end{aligned} \tag{5.16}$$

Inserting Eq.(5.16) into Eq.(5.7) yields,

$$u(\xi) = \mp\frac{2\sqrt{3\delta_2}m^2\left(-1 + dn(p\xi,m)^2\right)}{\lambda^2\sqrt{\rho}}. \tag{5.17}$$

The result obtained for Eq.(1.3) is

$$\phi(x,t) = -\frac{1}{\lambda}\ln\left[\mp\frac{2\sqrt{3\delta_2}m^2\left(-1 + dn(p\xi,m)^2\right)}{\lambda^2\sqrt{\rho}}\right]. \tag{5.18}$$

For $n \to 1$, the Eq.(5.18) becomes

$$\phi(x,t) = -\frac{1}{\lambda}\ln\left[\mp\frac{2\sqrt{3\delta_2}m^2\tanh^2(p\xi)}{\lambda^2\sqrt{\rho}}\right]. \tag{5.19}$$

The obtained solution represents dark soliton solutions and valid if $\rho > 0$ and $\delta_2 > 0$.
The value of ξ is defined in Eq.(5.2) for β-fractional and M-fractional derivative.

5.2 The tanh-coth expansion method

Balancing principle gives $N = 2$, then Eq.(4.1) becomes,

$$u(\xi) = A_0 + A_1\theta(\xi) + A_2\theta^2(\xi) + B_1\theta^{-1}(\xi) + B_2\theta^{-2}(\xi), \tag{5.20}$$

where A_0, A_1 and A_2 are the arbitrary parameters to be determined. The Eq.(5.7) is inserted along with the derivatives in Eq.(5.6). By assembling all the coefficients of $\theta(\xi)$ and equating them to zero, a system of algebraic equations is obtained. After solving the system with mathematica aid, the following sets of the solutions have been obtained.
For $\theta(\xi) = \tanh\xi$
Set 1
By employing the proposed technique the following values of parameters have been obtained.

$$\begin{aligned} A_0 &= \mp\frac{2\sqrt{3\delta_2}m^2}{\lambda^2\sqrt{\rho}}, \qquad A_1 = 0, \qquad A_2 = \mp\frac{2\sqrt{3\delta_2}m^2}{\lambda^2\sqrt{\rho}}, \\ B_1 &= 0, \qquad B_2 = 0, \qquad \mu = \mp\frac{\sqrt{\lambda^2(\delta_1 \mp 2\sqrt{3\rho\delta_2}) + 12m^2\delta_2}}{\lambda}, \\ C &= \mp\frac{4\left(\sqrt{3\delta_2}m^2\lambda^2\sqrt{\rho} - 3m^4\delta_2\right)}{\lambda^4}. \end{aligned} \tag{5.21}$$

Inserting Eq.(5.21) into Eq.(5.20) yields

$$u(\xi) = \mp\frac{2\sqrt{3\delta_2}m^2\left(-1+\coth(\xi)^2\right)}{\lambda^2\sqrt{\rho}}. \tag{5.22}$$

The obtained results for Eq.(1.3) is

$$\phi(x,t) = -\frac{1}{\lambda}\ln\left[\mp\frac{2\sqrt{3\delta_2}m^2 sech^2(\xi)}{\lambda^2\sqrt{\rho}}\right], \quad \rho > 0, \delta_2 > 0. \tag{5.23}$$

Eq.(5.23) represents the bright soliton solution for the proposed model.

Set 2

By employing the proposed technique the following values of parameters have been obtained.

$$\begin{aligned} A_0 &= \mp\frac{4\sqrt{3\delta_2}m^2}{\lambda^2\sqrt{\rho}}, \qquad A_1 = 0, \qquad A_2 = \mp\frac{2\sqrt{3\delta_2}m^2}{\lambda^2\sqrt{\rho}}, \\ B_1 &= 0, \qquad B_2 = \mp\frac{2\sqrt{3\delta_2}m^2}{\lambda^2\sqrt{\rho}}, \qquad \mu = \mp\frac{\sqrt{\lambda^2(\delta_1 \mp 2\sqrt{3\rho\delta_2}) + 48m^2\delta_2}}{\lambda}, \\ C &= \mp\frac{16\left(\sqrt{3\delta_2}m^2\lambda^2\sqrt{\rho} - 12m^4\delta_2\right)}{\lambda^4}. \end{aligned} \tag{5.24}$$

Inserting Eq.(5.24) into Eq.(5.20) yields

$$u(\xi) = \mp\frac{4\sqrt{3\delta_2}m^2}{\lambda^2\sqrt{\rho}} \mp \frac{2\sqrt{3\delta_2}m^2\left(\coth(\xi)^2\right)}{\lambda^2\sqrt{\rho}} \mp \frac{2\sqrt{3\delta_2}m^2\left(\tanh(\xi)^2\right)}{\lambda^2\sqrt{\rho}}. \tag{5.25}$$

The obtained solution for Eq.(1.3) is

$$\phi(x,t) = -\frac{1}{\lambda}\ln\left[\mp\frac{8\sqrt{3\delta_2}m^2\left(csch(\xi)^2\right)}{\lambda^2\sqrt{\rho}}\right]. \tag{5.26}$$

with constraint condition, $\rho > 0$ and $\delta_2 > 0$.

Set 3

By employing the proposed technique the following values of parameters have been obtained.

$$\begin{aligned} A_0 &= \mp\frac{2\sqrt{3\delta_2}m^2}{\lambda^2\sqrt{\rho}}, \qquad A_1 = 0, \qquad A_2 = 0, \\ B_1 &= 0, \qquad B_2 = \mp\frac{2\sqrt{3\delta_2}m^2}{\lambda^2\sqrt{\rho}}, \qquad \mu = \mp\frac{\sqrt{\lambda^2(\delta_1 \mp 2\sqrt{3\rho\delta_2}) + 12m^2\delta_2}}{\lambda}, \\ C &= \mp\frac{4\left(\sqrt{3\delta_2}m^2\lambda^2\sqrt{\rho} - 3m^4\delta_2\right)}{\lambda^4}. \end{aligned} \tag{5.27}$$

Inserting Eq.(5.27) into Eq.(5.20) yields

$$u(\xi) = \mp\frac{2\sqrt{3\delta_2}m^2\left(1-\tanh(\xi)^2\right)}{\lambda^2\sqrt{\rho}}. \tag{5.28}$$

The obtained solution for Eq.(1.3) is

$$\phi(x,t) = -\frac{1}{\lambda}\ln\left[\mp\frac{2\sqrt{3\delta_2}m^2\left(csch(\xi)^2\right)}{\lambda^2\sqrt{\rho}}\right]. \tag{5.29}$$

The soliton solutions are valid for $\rho > 0$ and $\delta_2 > 0$.

The value of ξ is defined in Eq.(5.2) for β-fractional and M-fractional derivative respectively.

6 Painlevé-test [22]

The algorithm for the Painlevé test is as follow:
Step 1 For investigating the dominant behavior, the following equation is inserted in Eq.(1.3),

$$\phi(x,t) = \alpha\theta^{\epsilon}(x,t), \tag{6.1}$$

where the ϵ indicates the dominant behavior that has been evaluated first, whereas, α is an arbitrary parameter.
Assuming

$$\phi(x,t) = \alpha_0\theta^{\epsilon}(x,t), \tag{6.2}$$

ϵ is substituted into Eq.(6.2) and the resulting equation is inserted into Eq.(1.3). Now α_0 is evaluated by equalizing the least power of $\theta(x,t)$ to zero.
Step 2 In order evaluate the resonances, it is assumed that

$$\phi(x,t) = \alpha_0\theta^{\epsilon}(x,t) + \alpha_r\theta^{\epsilon+r}(x,t). \tag{6.3}$$

The Eq.(6.3) is inserted into Eq.(1.3), then the sum of coefficients of α_r including lowest power of $\theta(x,t)$ is assembled. The resonances has been evaluated by the system of equations obtained by proposed technique.
Step 3 $\phi(x,t)$ can be expressed, as

$$\phi(x,t) = \theta^{\epsilon}(x,t)\sum_{i=0}^{r_m}\alpha_i\theta^{i}(x,t), \tag{6.4}$$

where r_m represents the maximum value of resonances and α_i represents the constant of integration. The Eq.(6.4) is substituted into Eq.(1.3) and α_i is evaluated for different level of r by equalizing the coefficients of powers of $\theta(x,t)$ to zero. The Painlevé-test is said to be satisfied if, the constants of integration α_r at the resonances $r_j,\ j=\ 1,\ 2,\ 3...$ becomes arbitrary constants.

6.1 Application of Painlevé test on proposed model

The Eq.(6.1) is inserted in Eq.(1.3), which yields

$$\begin{aligned}\alpha^4\Big(&-3\,\epsilon^3\left(\theta\left(x,t\right)\right)^{-4\,\epsilon-4}\left(\theta_x\left(x,t\right)\right)^4\delta_2+3\,\epsilon^3\left(\theta\left(x,t\right)\right)^{-4\,\epsilon-3}\left(\theta_x\left(x,t\right)\right)^2\theta_{1xx}\left(x,t\right)\delta_2\\&+2\left(\theta\left(x,t\right)\right)^{-6\,\epsilon}\lambda^4\alpha^2\rho-\epsilon\left(\theta\left(x,t\right)\right)^{-4\,\epsilon-2}\left(\theta_x\left(x,t\right)\right)^2\lambda^2\delta_1-2\left(\theta\left(x,t\right)\right)^{-5\,\epsilon}\lambda^4\alpha\,\rho\\&+\epsilon\left(\theta\left(x,t\right)\right)^{-4\,\epsilon-2}\left(\theta_t\left(x,t\right)\right)^2\lambda^2+\epsilon\left(\theta\left(x,t\right)\right)^{-4\,\epsilon-1}\theta_{xx}\left(x,t\right)\lambda^2\delta_1\\&-\epsilon\left(\theta\left(x,t\right)\right)^{-4\,\epsilon-1}\theta_{tt}\left(x,t\right)\lambda^2\Big).\end{aligned} \tag{6.5}$$

The value of ϵ is -2. Now ϵ is inserted into Eq.(6.2)

$$\phi(x,t) = \alpha_0\theta^{-2}(x,t). \tag{6.6}$$

Substituting Eq.(6.6) into Eq.(1.3) and equalizing the least power of $\theta(x,t)$ yields

$$\alpha_0 = \frac{2\sqrt{3\delta_2}\left(\theta_x\left(x,t\right)\right)^2}{\lambda^2\sqrt{\rho}}. \tag{6.7}$$

Substituting ϵ and α_0, the Eq.(6.3) becomes

$$\phi(x,t) = \frac{2\sqrt{3\delta_2}\left(\theta_x\left(x,t\right)\right)^2}{\lambda^2\sqrt{\rho}}\theta^{-2}(x,t) + \alpha_s\theta^{s-2}(x,t). \tag{6.8}$$

Substituting Eq.(6.8) in Eq.(1.3) and equalizing the sum of coefficients of α_r by equaling the least power of $\theta(x,t)$ to zero, the following expression has been obtained.

$$1152\sqrt{3}\sqrt{\delta_2\left(\theta_x\left(x,t\right)\right)^4}{\delta_2}^2\left(\theta_x\left(x,t\right)\right)^8+864\sqrt{3}\sqrt{\delta_2\left(\theta_x\left(x,t\right)\right)^4}{\delta_2}^2\left(\theta_x\left(x,t\right)\right)^8 r$$
$$-288\sqrt{\delta_2\left(\theta_x\left(x,t\right)\right)^4}{\delta_2}^2\left(\theta_x\left(x,t\right)\right)^8 r^2=0. \tag{6.9}$$

Eq.(6.9) becomes

$$1152\sqrt{3}+864\sqrt{3}r-288r^2=0. \tag{6.10}$$

Solving for r gives

$$r_1=-1,\quad r_2=4. \tag{6.11}$$

Determine the compatibility condition, inserting ϵ and maximum value of resonances $s=r_m=4$ in Eq.(6.4)

$$\phi(x,t)=\theta^{-2}(x,t)\sum_{r=0}^{4}\alpha_r\theta^r(x,t). \tag{6.12}$$

Eq.(6.12) is substituted into Eq.(1.3). The value of constants of integration α_r, $r=1,\ 2,\ 3,\ 4$ have been evaluated by equalizing the coefficients of least powers of $\theta(x,t)$ to zero.
For $r=1$,

$$\alpha_1=\frac{-2}{\lambda^2}\frac{\sqrt{3\delta_2}}{\sqrt{\rho}}\theta_{xx}(x,t). \tag{6.13}$$

Similarly, at $r=2$,

$$\begin{aligned}\alpha_2 \;=\; & \frac{\sqrt{3}}{288\left(\theta_x\left(x,t\right)\right)^2\lambda^2\rho\sqrt{\delta_2}}\Big(32\sqrt{3}\left(\theta_x\left(x,t\right)\right)^2\lambda^2\rho\sqrt{\delta_2}\\ & +16\left(\theta_x\left(x,t\right)\right)^2\lambda^2\sqrt{\rho}\delta_1-16\left(\theta_t\left(x,t\right)\right)^2\lambda^2\sqrt{\rho}+192\,\theta_x\left(x,t\right)\theta_{xxx}\left(x,t\right)\sqrt{\rho}\delta_2\\ & -219\left(\theta_{xx}\left(x,t\right)\right)^2\sqrt{\rho}\delta_2\Big).\end{aligned} \tag{6.14}$$

Likewise, at $r=3$,

$$\begin{aligned}\alpha_3 \;=\; & -\frac{\sqrt{3}}{1152\,{\delta_2}^{5/2}\left(\theta_x\left(x,t\right)\right)^4\lambda^2\rho^3}\Big(880\,{\delta_2}^{5/2}\left(\theta_x\left(x,t\right)\right)^2\theta_{xx}\left(x,t\right)\sqrt{3}\lambda^2\rho^3\\ & -96\,\theta_{tt}\left(x,t\right){\delta_2}^2\left(\theta_x\left(x,t\right)\right)^2\lambda^2\rho^{5/2}-464\left(\theta_t\left(x,t\right)\right)^2{\theta_2}^2\theta_{xx}\left(x,t\right)\lambda^2\rho^{5/2}\\ & +560\left(\theta_x\left(x,t\right)\right)^2\theta_{xx}\left(x,t\right)\rho^{5/2}\lambda^2{\delta_2}^2p_1+8448\,{\delta_2}^3\theta_x\left(x,t\right)\theta_{xx}\left(x,t\right)\theta_{xxx}\left(x,t\right)\rho^{5/2}\\ & -10833\,{\delta_2}^3\left(\theta_{xx}\left(x,t\right)\right)^3\rho^{5/2}\Big).\end{aligned} \tag{6.15}$$

In the similar way, at $r=4$,

$$\alpha_4=\alpha_4. \tag{6.16}$$

After satisfying the compatibility conditions, it is proved that the proposed model is integrable.

7 Graphical illustration

This section contains the 3D and 2D plots of some of the obtained solutions for studying fractional impact. The graphical representations of Eq.(5.11) have been carried out in Fig.(7.1), Fig.(7.2) and Fig.(7.3) by assuming the values of arbitrary parameters as $\lambda=6.33$, $\rho=1.0$, $\delta_1=-15.0$, $\delta_2=1.0$, $a=2.0$, $\tau=0.70$ and fractional parameter $\gamma=0.45$, $\gamma=0.75$ and $\gamma=0.95$, respectively.

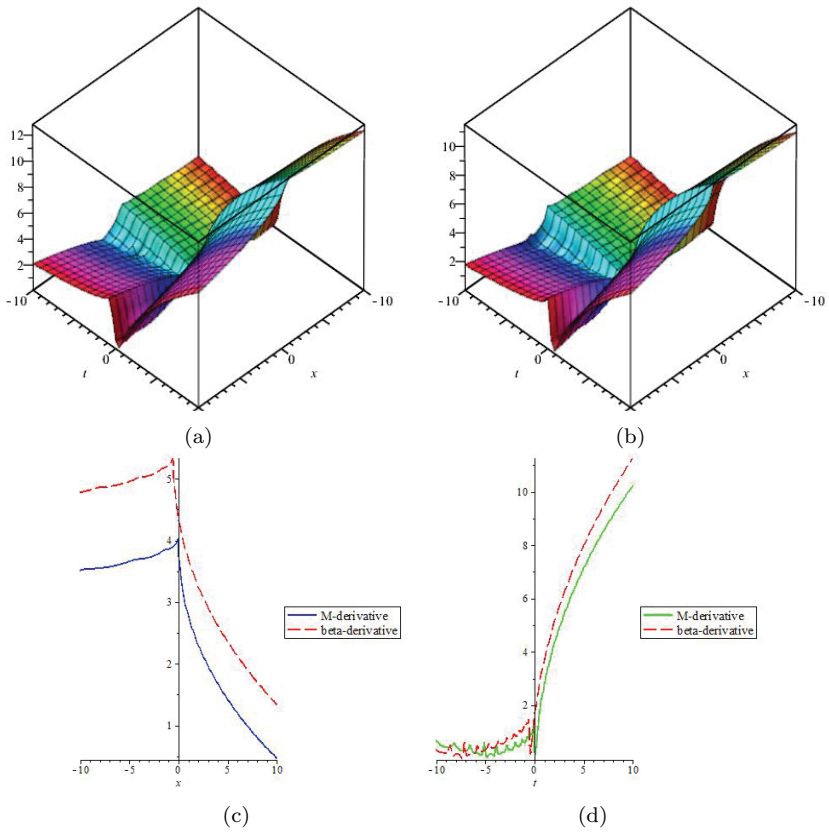

Figure 7.1: (a) 3D plot w.r.t β-derivative ,(b) 3D plot w.r.t M-derivative,(c) is **2D line graph** with the variation in x ,(d) is **2D line graph** with the variation in t of Eq.(5.11) where the fractional operator $\gamma = 0.45$.

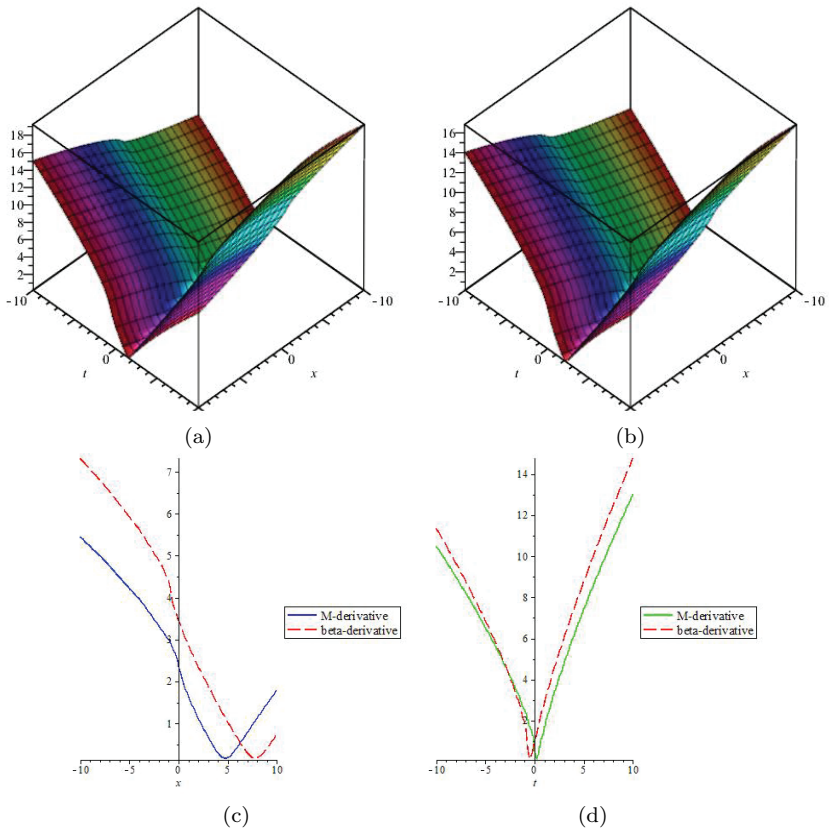

Figure 7.2: (a) 3D plot w.r.t β-derivative ,(b) 3D plot w.r.t M-derivative,(c) is **2D line graph** with the variation in x ,(d) is **2D line graph** with the variation in t of Eq.(5.11) where the fractional operator $\gamma = 0.75$.

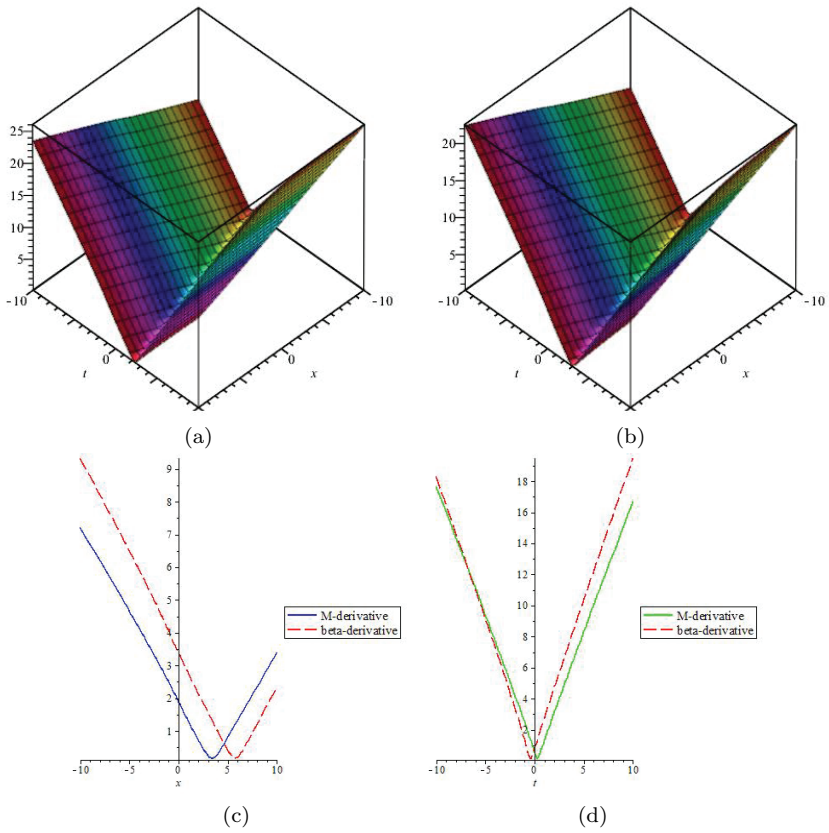

Figure 7.3: (a) 3D plot w.r.t β-derivative ,(b) 3D plot w.r.t M-derivative,(c) is **2D line graph** with the variation in x ,(d) is **2D line graph** with the variation in t of Eq.(5.11) where the fractional operator $\gamma = 0.95$.

The graphical representations of Eq.(5.15) have been carried out in Fig.(7.4), Fig.(7.5) and Fig.(7.6) by assuming the values of arbitrary parameters as $\lambda = 6.33$, $\rho = 1.0$, $\delta_1 = -15.0$, $\delta_2 = 1.0$, $a = 2.0$, $\tau = 0.70$ and fractional parameter $\gamma = 0.45$, $\gamma = 0.75$ and $\gamma = 0.95$, respectively.

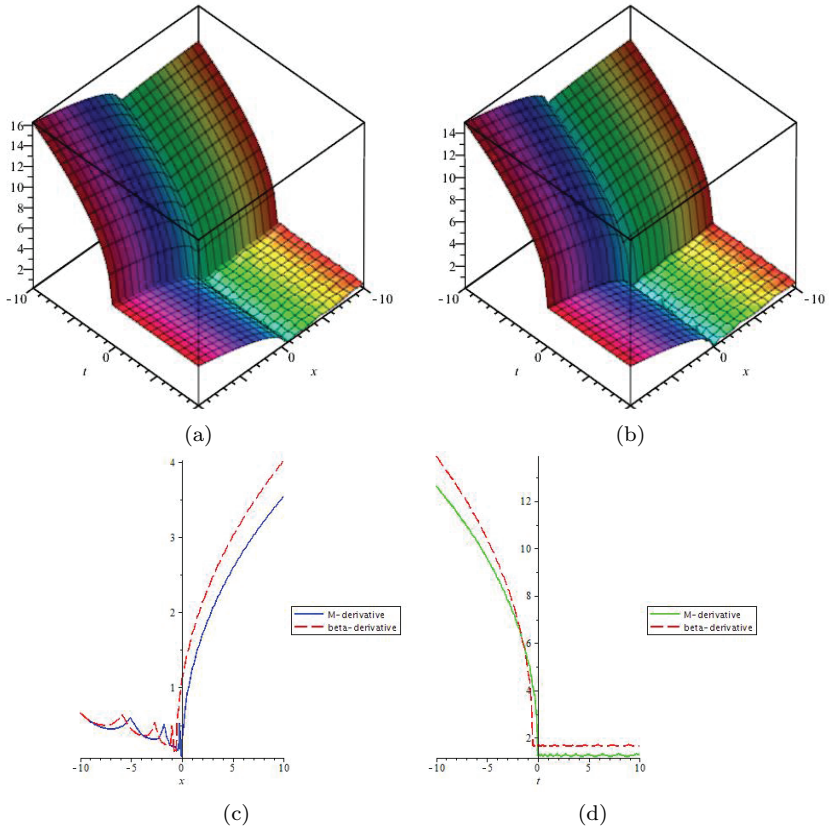

Figure 7.4: (a) 3D plot w.r.t β-derivative ,(b) 3D plot w.r.t M-derivative,(c) is **2D line graph** with the variation in x ,(d) is **2D line graph** with the variation in t of Eq.(5.15) where the fractional operator $\gamma = 0.45$.

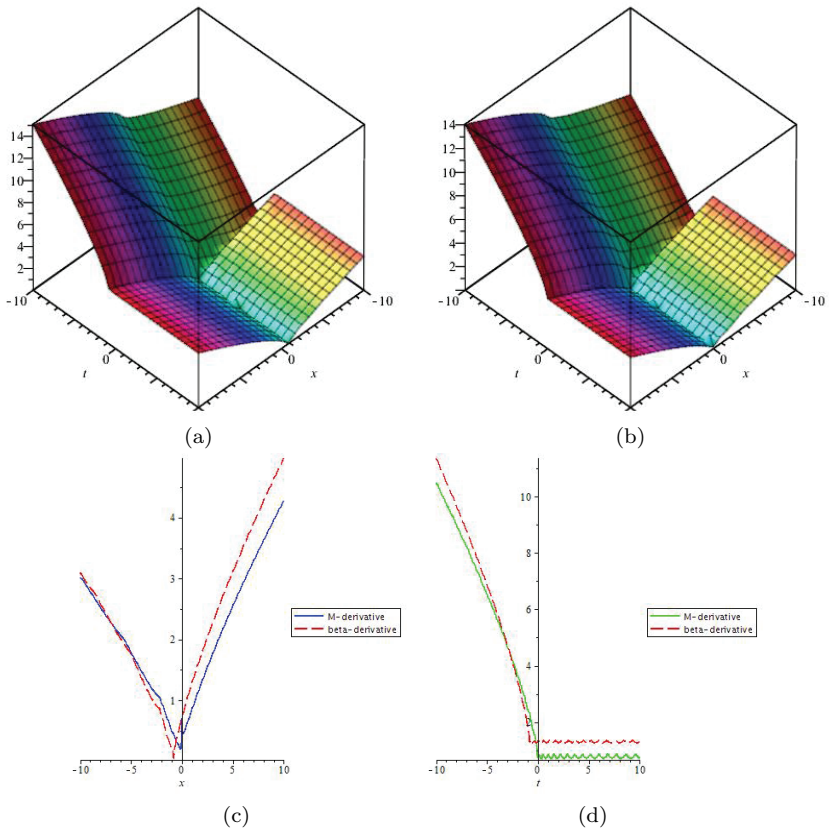

Figure 7.5: (a) 3D plot w.r.t β-derivative ,(b) 3D plot w.r.t M-derivative,(c) is **2D line graph** with the variation in x ,(d) is **2D line graph** with the variation in t of Eq.(5.15) where the fractional operator $\gamma = 0.75$.

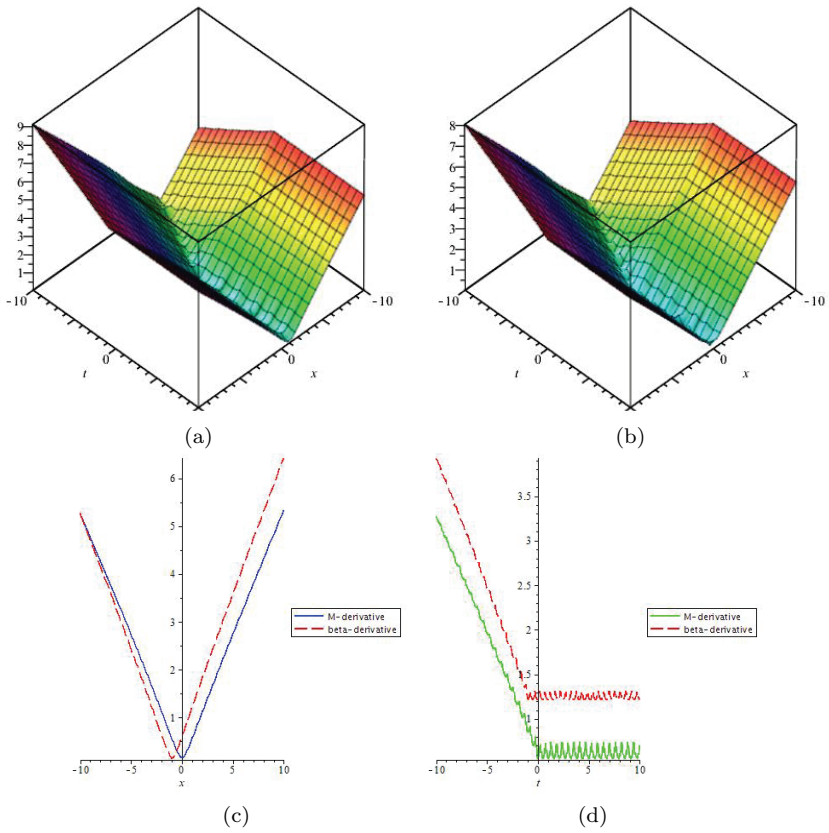

Figure 7.6: (a)3D plot w.r.t β-derivative ,(b) 3D plot w.r.t M-derivative,(b) is **3D graph** w.r.t M-derivative,(c) is **2D line graph** with the variation in x ,(d) is **2D line graph** with the variation in t of Eq.(5.15) where the fractional operator $\gamma = 0.95$.

The graphical representations of Eq.(5.23) have been carried out in Fig.(7.7), Fig.(7.8) and Fig.(7.9) by assuming the values of arbitrary parameters as $\lambda = 6.33$, $\rho = 1.0$, $\delta_1 = -15.0$, $\delta_2 = 1.0$, $a = 2.0$, $\tau = 0.70$ and fractional parameter $\gamma = 0.45$, $\gamma = 0.75$ and $\gamma = 0.95$, respectively.

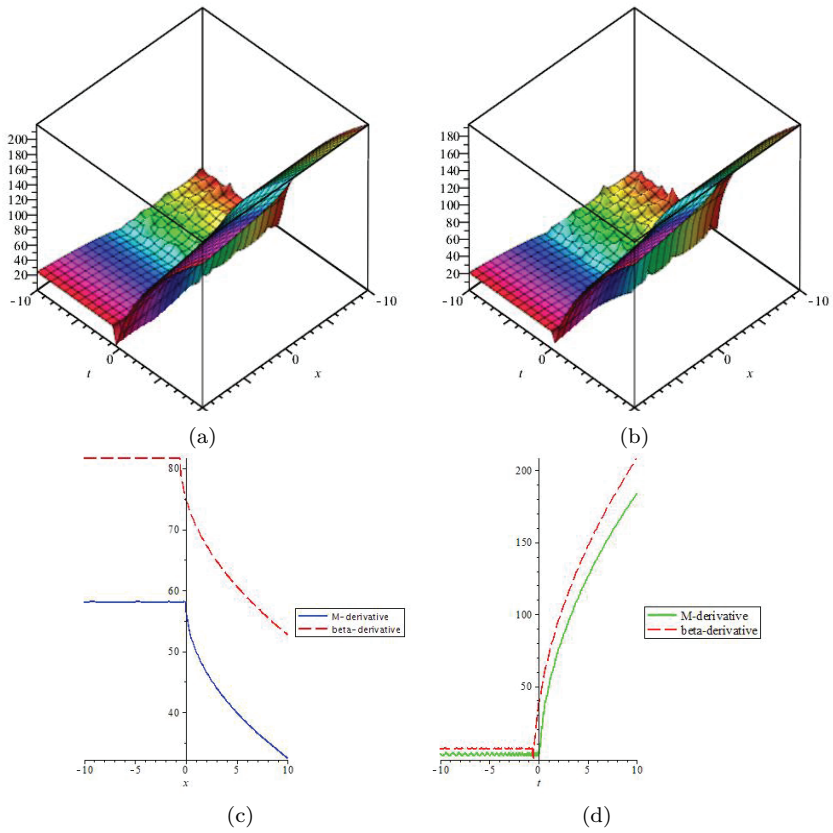

Figure 7.7: (a) 3D plot w.r.t β-derivative ,(b) 3D plot w.r.t M-derivative,(c) is **2D line graph** with the variation in x ,(d) is **2D line graph** with the variation in t of Eq.(5.23) where the fractional operator $\gamma = 0.5$.

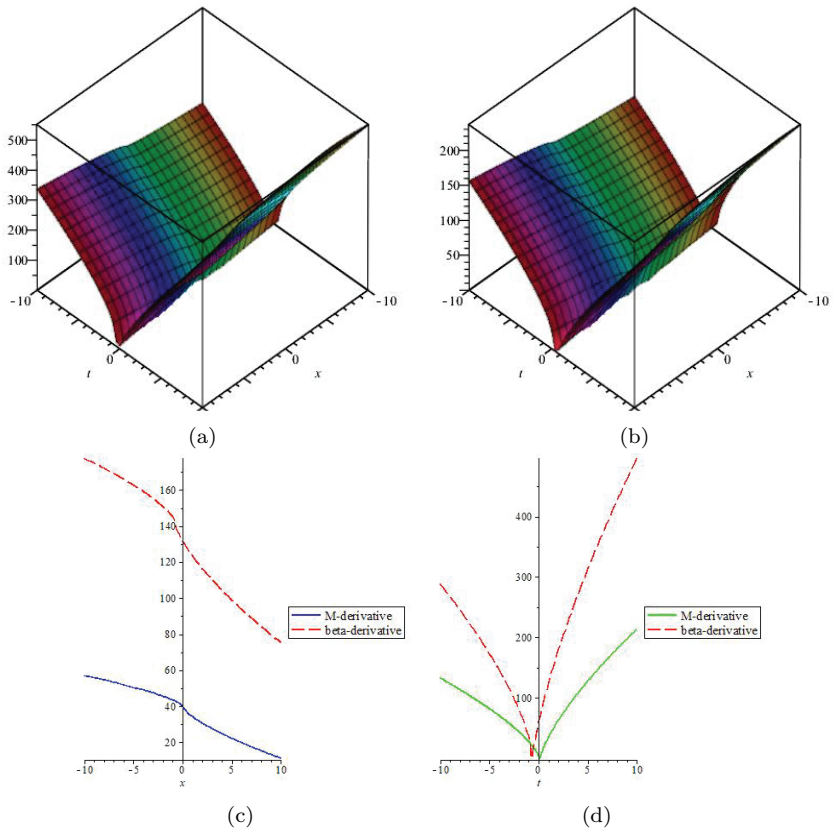

Figure 7.8: (a) 3D plot w.r.t β-derivative ,(b) 3D plot w.r.t M-derivative,(c) is **2D line graph** with the variation in x ,(d) is **2D line graph** with the variation in t of Eq.(5.23) where the fractional operator $\gamma = 0.7$.

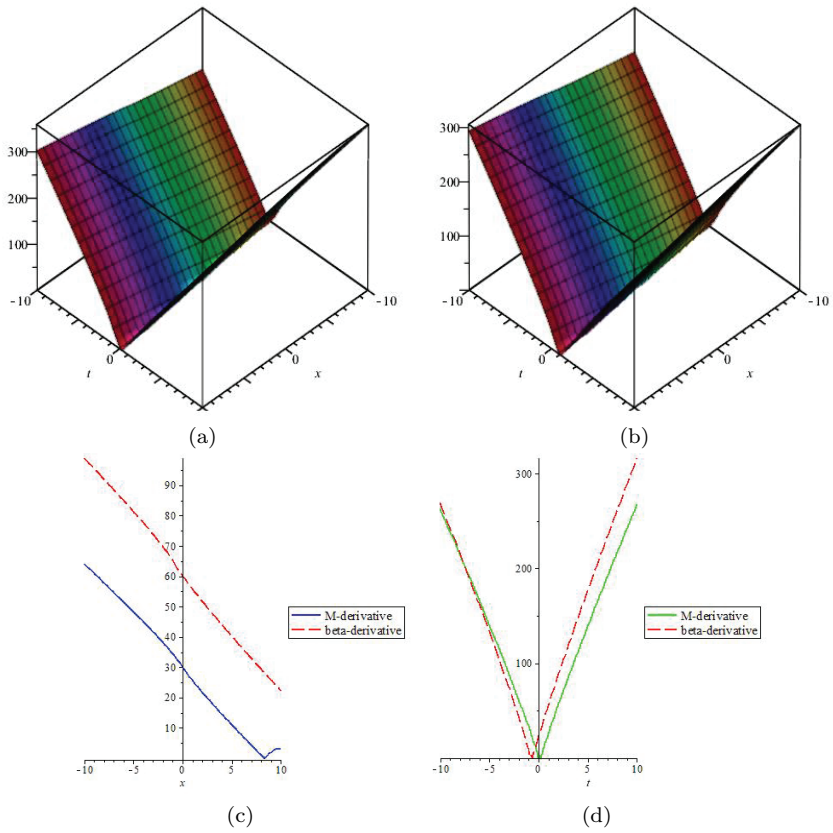

Figure 7.9: (a) 3D plot w.r.t β-derivative ,(b) 3D plot w.r.t M-derivative,(c) is **2D line graph** with the variation in x ,(d) is **2D line graph** with the variation in t of Eq.(5.23) where the fractional operator $\gamma = 0.9$.

8 Conclusion

This paper addresses the fractional Peyrard-Bishop DNA model. The β-derivative and M-truncated derivative are employed in this article for studying the fractional behavior of the model. These fractional derivatives have significant importance in investigating the memory and heredity properties of the problems found in science and engineering. The proposed fractional model is solved using JEFM and $\tanh - \coth$ expansion method for the first time in this article. Some constructed solutions are plotted graphically by assigning particular values of arbitrary parameters. Moreover, the Painlevé-test is applied to confirm that the proposed model is integrable.

References

[1] M.A. Agüero, M.A.D.L. Najera, and M. Carrillo. Nonclassic solitonic structures in DNA's vibrational dynamics. *International Journal of Modern Physics B*, 22(16):2571–2582, 2008.

[2] G. Akram, S. Arshed, and Z. Imran. Soliton solutions for fractional DNA Peyrard-Bishop equation via the extended $\left(\frac{G'}{G^2}\right)$-expansion method. *Physica Scripta*, 96(9):094009, 2021.

[3] K.K. Ali, C. Cattani, J.F. Gómez-Aguilar, D. Baleanu, and M.S. Osman. Analytical and numerical study of the DNA dynamics arising in oscillator-chain of Peyrard-Bishop model. *Chaos, Solitons & Fractals*, 139:110089, 2020.

[4] A. Atangana, D. Baleanu, and A. Alsaedi. Analysis of time-fractional Hunter-Saxton equation: a model of neumatic liquid crystal. *Open Physics*, 14(1):145–149, 2016.

[5] S. Bibi, S.T. Mohyud-Din, R. Ullah, N. Ahmed, and U. Khan. Exact solutions for STO and (3+1)-dimensional KdV-ZK equations using $\frac{G'}{G^2}$-expansion method. *Results in Physics*, 7:4434–4439, 2017.

[6] A. Biswas, M. Ekici, A. Sonmezoglu, and M.R. Belic. Highly dispersive optical solitons with Kerr law nonlinearity by extended Jacobi's elliptic function expansion. *Optik: International Journal for Light and Electron Optics*, 183:395–400, 2019.

[7] F. Blaschke, O.N. Karpíšek, and P. Beneš. Solitons in the Peyrard-Bishop model of DNA and the renormalization group method. *Progress of Theoretical and Experimental Physics*, 2020(6):063J02, 2020.

[8] R.F. Camargo and E.C. de Oliveira. Fractional calculus (in portuguese). *Editora Livraria da Física, São Paulo*, 2015.

[9] T. Dauxois. Dynamics of breather modes in a nonlinear helicoidal model of DNA. *Physics Letters A*, 159(8-9):390–395, 1991.

[10] E.C. de Oliveira and J.A.T. Machado. A review of definitions for fractional derivatives and integral. *Mathematical Problems in Engineering*, 2014:238459, 2014.

[11] B. Ghanbari and J.F. Gómez-Aguilar. The generalized exponential rational function method for Radhakrishnan-Kundu-Lakshmanan equation with β-conformable time derivative. *Revista Mexicana de Física*, 65(5):503–518, 2019.

[12] U.N. Katugampola. A new fractional derivative with classical properties. *rXiv preaprint arXiv:1410.6535*, 2014.

[13] S. Liu, Z. Fu, S. Liu, and Q. Zhao. Jacobi elliptic function expansion method and periodic wave solutions of nonlinear wave equations. *Physics Letters A*, 289(1-2):69–74, 2001.

[14] J. Manafian, O.A. Ilhan, and S.A. Mohammed. Forming localized waves of the nonlinearity of the DNA dynamics arising in oscillator-chain of Peyrard-Bishop model. *AIMS Mathematics*, 5(3):2461–2483, 2020.

[15] S.T. Mohyud-Din and S. Bibi. Exact solutions for nonlinear fractional differential equations using $(\frac{G'}{G^2})$-expansion method. *Alexandria Engineering Journal*, 57(2):1003–1008, 2018.

[16] V. F. Morales-Delgado, J. F. Gómez-Aguilar, and M. A. Taneco-Hernandez. Analytical solutions of electrical circuits described by fractional conformable derivatives in Liouville-Caputo sense. *AEU-International Journal of Electronics and Communications*, 85:108–117, 2018.

[17] L. Najera, M. Carrillo, and M.A. Aguero. Non-classical solitons and the broken hydrogen bonds in DNA vibrational dynamics. *Advanced Studies in Theoretical Physics*, 4:495–510, 2010.

[18] E. J. Parkes. Observations on the tanh-coth expansion method for finding solutions to nonlinear evolution equations. *Applied Mathematics and Computation*, 217(4):1749–1754, 2010.

[19] M. Peyrard and A.R. Bishop. Statistical mechanics of a nonlinear model for DNA denaturation. *Physical Review Letters*, 62(23):2755, 1989.

[20] I. Podlubny. Fractional differential equations, mathematics in science and engineering. *Academic Press, San Diego*, 1999.

[21] S. T. R. Rizvi, K. Ali, S. Bashir, M. Younis, R. Ashraf, and M. O. Ahmad. Exact soliton of (2+1)-dimensional fractional Schrödinger equation. *Superlattices and Microstructures*, 107:234–239, 2017.

[22] S. T. R. Rizvi, A. R. Seadawy, M. Younis, I. Ali, S. Althobaiti, and S. F. Mahmoud. Soliton solutions, Painleve analysis and conservation laws for a nonlinear evolution equation. *Results in Physics*, 23:103999, 2021.

[23] S. Salahshour, A. Ahmadian, S. Abbasbandy, and D. Baleanu. M-fractional derivative under interval uncertainty: Theory, properties and applications. *Chaos, Solitons & Fractals*, 117:84–93, 2018.

[24] J. V. D. C. Sousa and E. C. de Oliveira. A new truncated M-fractional derivative type unifying some fractional derivative types with classical properties. *International Journal of Analysis and Application*, 16(1):83–96, 2018.

[25] J.V.D.C. Sousa and E.C. de Oliveira. On the local m-derivative. *Progress in Fractional Differentiation and Applications*, 4:479–492, 2018.

[26] A. Zafar, K.K. Ali, M. Raheel, N. Jafar, and K.S. Nisar. Soliton solutions to the DNA Peyrard-Bishop equation with beta-derivative via three distinctive approaches. *The European Physical Journal Plus*, 135(9):1–17, 2020.

[27] S. Zdravković. Helicoidal Peyrard-Bishop model of DNA dynamics. *Journal of Nonlinear Mathematical Physics*, 18(sup2):463–484, 2011.